



Published in final edited form as:

*J Chem Theory Comput.* 2009 September 8; 5(9): 2301–2312. doi:10.1021/ct900344g.

## Through-Space Effects of Substituents Dominate Molecular Electrostatic Potentials of Substituted Arenes

Steven E. Wheeler\* and K. N. Houk\*

Department of Chemistry and Biochemistry University of California, Los Angeles, CA 90095

### Abstract

Model systems have been studied using density functional theory to assess the contributions of  $\pi$ -resonance and through-space effects on electrostatic potentials of substituted arenes. The results contradict the widespread assumption that changes in molecular ESPs reflect only local changes in the electron density. Substituent effects on the ESP above the molecular plane are commonly attributed to changes in the aryl  $\pi$ -system. We show that ESP changes for a collection of substituted benzenes and more complex aromatic systems can be accounted for mostly by through-space effects, with no change in the aryl  $\pi$ -electron density. Only when  $\pi$ -resonance effects are substantial do they influence changes in the ESP above the aromatic ring to any extent. Examples of substituted arenes studied here are taken from the fields of drug design, host-guest chemistry, and crystal engineering. These findings emphasize the potential pitfalls of assuming ESP changes reflect changes in the local electron density. Since ESP changes are frequently used to rationalize and predict intermolecular interactions, these findings have profound implications for our understanding of substituent effects in countless areas of chemistry and molecular biology. Specifically, in many non-covalent interactions there are significant, often neglected, through-space interactions with the substituents. Finally, the present results explain the perhaps unexpectedly good performance of many molecular mechanics force-fields applied to supramolecular assembly phenomena and  $\pi$ - $\pi$  interactions in biological systems despite the neglect of the polarization of the aryl  $\pi$ -system by substituents.

### I. Introduction

Molecular electrostatic potentials (ESPs) have emerged as powerful predictive and interpretive tools in disparate areas of chemistry, rational drug design, and molecular biology.<sup>1,2</sup> Colorful plots of ESPs have been used to rationalize trends in organic reactivity<sup>3</sup> and binding in host-guest complexes and non-covalent interactions (cation/ $\pi$ ,  $\pi$ - $\pi$ , *etc.*).<sup>4–9</sup> Information gleaned from ESPs is often utilized in analyses of protein-ligand and protein-protein interactions,<sup>10</sup> as well as studies of the folding of model proteins.<sup>11</sup> Quantitative ESP-based reactivity descriptors have also emerged, offering alternatives to traditional substituent constants.<sup>12</sup> Computed ESPs have even been correlated with impact sensitivities of explosive compounds<sup>13</sup> and toxicity in polychlorinated biphenyls (PCBs).<sup>14</sup> Moreover, ESPs can be readily computed using standard electronic structure theory packages or derived from experimental X-ray diffraction data,<sup>15</sup> providing a simple, easily accessible tool for understanding numerous phenomena.

The electrostatic potential at a given point near a molecule is a measure of the electrostatic energy a positive unit test charge would experience at that point. Negative ESPs correspond to an attractive interaction with this positive test charge while positive ESPs indicate repulsion.

\*swheele2@chem.ucla.edu, houk@chem.ucla.edu.

**Supporting Information Available:** Plots comparing ESPs at different levels of theory and with and without geometry constraints.

Non-uniform electrostatic potentials arise in molecular environments from the competing effects of the nuclear charges and the surrounding electrons. The use of ESPs to predict and rationalize reactivity trends was pioneered by Scrocco, Tomasi and coworkers,<sup>16</sup> who studied electrophilic attack of three-membered rings and nucleic acid bases and proton affinities of amides. Subsequently, ESP plots have been applied to sundry chemical systems, driven in large part by the many reports of Politzer and Murray.<sup>2,3</sup> ESP plots also enjoy wide applicability in the analysis of non-covalent interactions. They have been used in the development of conceptual models of the electrostatic component of prototypical interactions and provide a simple means of approximating the interaction strength and geometry of non-covalent complexes.<sup>4–9</sup> ESPs have been applied to non-covalent interactions of increasingly complex systems, culminating in studies of protein-ligand and protein-protein interactions.<sup>4</sup>

Unfortunately, the literature is peppered with false assumptions regarding the effect of substituents on ESPs. It is common to equate changes in the ESP in a given region with *local* changes in the electron density. For example, in a recent study of non-covalent interactions in mechanically interlocked compounds, Goddard, Stoddart, and co-workers<sup>17</sup> used ESP plots to evaluate electron density differences of the central naphthalene core for a series of substituted systems. Indeed, when presenting ESP plots, many authors explicitly label regions of negative electrostatic potential “electron-rich” and positive ESP regions “electron-poor”.<sup>18</sup> This connection between ESP values and the local electron density is also advanced in otherwise stellar textbooks on physical organic chemistry<sup>19</sup> and in publications advocating the use of ESP plots in undergraduate education.<sup>20</sup> Politzer and Murray<sup>3</sup> emphasized nearly two decades ago that the ESP is the “net result at a given point of the integrated effects of all of the electrons and nuclei, whereas  $\rho(\mathbf{r})$  of course represents only the electronic density at that point.” While negative ESPs often do correspond to electron-rich regions, the assumption that changes in ESPs necessarily indicate local changes in the electron density is incorrect.

The gas-phase ESP at a given point,  $V(\mathbf{r})$ , is defined by eq (1), where  $Z_A$  and  $\mathbf{R}_A$  are the charge and position of nucleus A, respectively, and  $\rho(\mathbf{r}')$  is the electron density at position  $\mathbf{r}'$ , all in atomic units.

$$V(\mathbf{r}) = \sum_A^{\text{nuclei}} \frac{Z_A}{|\mathbf{r} - \mathbf{R}_A|} - \int \frac{\rho(\mathbf{r}')}{|\mathbf{r} - \mathbf{r}'|} d\mathbf{r}' \quad (1)$$

The integral in eq (1) runs over all space. Thus, at a given point the ESP is dependent on the electron density in all surrounding space, though this dependency dies off with distance. Despite this  $1/r$  dependence, seemingly subtle changes in the electron density several angstroms away can have profound effects on the ESP at a given point. For example, a charge of  $0.1e$  contributes more than  $10 \text{ kcal mol}^{-1}$  to the ESP at a distance of three Angstroms.

Substituent effects on aromatic rings have been studied extensively since the pioneering work of Hammett.<sup>21</sup> Generally, the effects of a substituent on an aryl ring are transmitted via numerous potential mechanisms, which are often conceptually divided into  $\pi$ -resonance, inductive (through- $\sigma$ -bond), and field (through-space) effects.<sup>22</sup> There have been numerous attempts to quantify these often competing effects, leading to the development of a bevy of substituent constants.<sup>23</sup> Among the most popular separations of  $\pi$ - and  $\sigma$ -effects comes from the work of Roberts and Moreland,<sup>24</sup> Taft,<sup>25</sup> and Swain and Lupton,<sup>26</sup> who partitioned substituent constants into resonance effects (as quantified by  $\sigma_R$  or  $R$ ) and inductive/field effects ( $\sigma_I$  or  $F$ ). In these schemes, more negative numbers indicate stronger electron donating tendency while more positive values correspond to stronger electron acceptors. Substituent effects arise from some combination of resonance and inductive/field effects, with the relative

contribution varying with the substituent. ESP maps of substituted benzenes should similarly reflect both  $\pi$ -resonance and inductive/field effects.

The potentially large contribution of through-space substituent effects is mostly absent in discussions of ESPs of substituted arenes in the modern literature. Many authors assume changes in arene ESPs reflect donation into or out of the aryl  $\pi$ -system. For example, in their extensive studies of substituent effects on the benzene dimer,<sup>8,9,27–29</sup> Sherrill and coworkers utilized ESP plots to characterize the “degree of  $\pi$ -density” in substituted benzenes. This idea is appealing, since it enables simple resonance-based explanations of trends in electrostatic potential plots. That is, the ESP above benzene substituted with an electron-withdrawing group will generally be more positive than that of benzene, rationalized based on resonance forms with a formal positive charge at the *ortho* and *para* positions. More negative ESPs above benzenes substituted with electron donors are often explained by resonance forms with a negative charge on the benzene ring.

Two subtle exceptions to such  $\pi$ -resonance-based explanations of ESPs are phenol and anisole. Based on Hammett substituent constants, OH and OMe are  $\pi$ -electron-donating substituents [ $R(\text{OCH}_3) = -0.56$ ,  $R(\text{OH}) = -0.70$ ],<sup>23</sup> so the ESPs above the aryl ring in these two systems should be more negative than in benzene according to the simple  $\pi$ -resonance picture. However, the ESPs above phenol and anisole are slightly more positive than that of benzene (see Fig. 1a–c). Analogously, the interaction of  $\text{Na}^+$  with  $\text{C}_6\text{H}_5\text{OH}$  and  $\text{C}_6\text{H}_5\text{OCH}_3$  is slightly weaker than the  $\text{Na}^+\cdots\text{C}_6\text{H}_6$  interaction.<sup>5,30,31</sup> This seemingly counterintuitive phenomenon has been mentioned previously,<sup>27,30,32</sup> most prominently by Dougherty and co-workers<sup>5,30</sup> who noted that the strength of cation/ $\pi$  interactions and the ESP above the center of substituted benzenes are more strongly correlated with  $\sigma_m$  constants than  $\sigma_p$ . Hunter and co-workers<sup>7</sup> also reported a strong correlation between  $\sigma_m$  and the ESP at the centroid of substituted aromatic rings. This  $\sigma_m$ -dependence is contrary to the prevalent  $\pi$ -resonance-based explanations of ESPs of substituted arenes, since  $\sigma_m$  constants reflect mostly non-resonance effects. In the case of phenol and anisole, the  $\sigma$ -withdrawing effect on the ESP overwhelms the  $\pi$ -donation, as noted by Klärner and co-workers.<sup>32</sup>

A more clear-cut example of the dominant role of inductive/field effects on ESPs was provided by Politzer and co-workers in 1987.<sup>33</sup> The ESP map of nitrobenzene is positive everywhere above the aryl plane, a feature which might naively be attributed to  $\pi$ -electron-withdrawal. However, Politzer *et al.*<sup>33</sup> showed that the ESP of nitrobenzene is essentially unchanged upon a  $90^\circ$  rotation of the nitro group (see Fig. 1d). In perpendicular nitrobenzene there can be no  $\pi$ -resonance between  $\text{NO}_2$  and the aryl  $\pi$ -system, yet the ESP is still positive everywhere above the benzene plane. Clearly, in nitrobenzene  $\pi$ -resonance has little net effect on the ESP; substituent effects on the ESP must arise from inductive/field effects. This finding is consistent with the typical characterization of  $\text{NO}_2$  as a strong inductive electron withdrawing group but modest resonance acceptor ( $F = 0.65$ ,  $R = 0.13$ ).<sup>23</sup>

Substituent effects on the electrostatic properties of aromatic systems are central to many areas of modern chemistry and molecular biology and maps of molecular electrostatic potentials constitute a powerful and popular tool for rationalizing and predicting non-covalent interactions. Consequently, a full understanding of chemical and biochemical systems must rest on a sound understanding of the changes in ESPs induced by substituents. Previously, we demonstrated<sup>31</sup> that substituent effects on the ESP at a point approximately  $2.4 \text{ \AA}$  above the center of monosubstituted benzenes arise primarily from direct through-space effects of the substituents, and  $\pi$ -resonance effects play a relatively minor role. We now show that for a wide range of substituents, changes in ESP maps of substituted aromatic systems are generally dominated by through-space effects of the substituents. More importantly, the widespread,

often implicit assumption that changes in ESPs necessarily indicate *local* changes in electron density is shown to be unfounded and in many cases misleading.

## II. Theoretical Methods

The molecular electrostatic potential,  $V(\mathbf{r})$ , was evaluated on a rectangular grid enveloping each molecule according to eq (1) and using electron densities computed at the B3LYP/6-31G(d) level of theory<sup>34</sup> with Gaussian03.<sup>35</sup> These ESP plots are relatively insensitive to the method and basis set employed, as demonstrated for cyanobenzene in Supporting Information (SI, see Fig. S1). Graphical representations of these ESPs were generated by mapping the ESP onto a molecular surface corresponding to an isodensity contour at  $\rho = 0.005$  or  $0.001 \text{ e/au}^3$  using UCSF Chimera.<sup>36</sup> The wide range of systems considered necessitated the use of several different scales for plotted ESPs. The scales utilized are displayed in each figure, and within a given figure the ESP scale is always the same to facilitate straightforward comparisons of different systems.

An additive ESP model was employed to differentiate between  $\pi$ -resonance and inductive/field effects, constructed as follows for monosubstituted benzenes: for each point on an identical rectangular grid, the ESP was evaluated for  $\text{C}_6\text{H}_6$ ,  $\text{C}_6\text{H}_5\text{X}$ , and  $\text{HX}$ , with each system positioned so that conserved atoms were placed identically. For example, for fluorobenzene all six carbons and the five unsubstituted hydrogens have the same Cartesian coordinates in  $\text{C}_6\text{H}_6$  as  $\text{C}_6\text{H}_5\text{F}$ . The fluorines in  $\text{C}_6\text{H}_5\text{F}$  and  $\text{HF}$  also have identical coordinates. The positions of the substituted atoms were optimized. These constraints result in no discernible difference in ESP plots, as demonstrated in SI Fig. S2. The ESPs of  $\text{C}_6\text{H}_6$  and  $\text{HX}$  were then added at each point on this grid, and the resulting additive ESP mapped onto the electron density isosurface of  $\text{C}_6\text{H}_5\text{X}$ .<sup>37</sup> To provide a quantitative measure of the similarity of the additive and true ESPs, the Hodgkin index,<sup>38</sup>  $\mathbf{H}$ , has been computed for the ESP values on the plotted isodensity surfaces. The Hodgkin index for two sets of ESP values ranges from  $-1.00$ , for two equal but opposite ESP values, to  $1.00$  for identical ESPs.

## III. Plots of Molecular Electrostatic Potentials

### A. Substituted Benzenes

Monosubstituted benzenes serve as models for more complex substituted aromatic systems, and without understanding the effect of substituents in these paradigmatic systems there is little hope for a sound analysis of more complex substituted arenes. Standard ESP plots are provided for 20 substituted benzenes in Fig. 2 (first and third rows). ESP plots for four aniline derivatives are shown in the top row of Fig. 3. These ESP plots show the expected qualitative trends: electron-withdrawing substituents generally increase the ESP above the aryl ring while donors lead to a decrease in the ESP, relative to benzene. These ESP maps reflect both  $\pi$ -resonance and inductive/field effects, the relative contribution of which cannot be discerned from these plots alone.

To assess the role of non-resonance effects, ESPs from an additive model for each of these species are also plotted in Fig. 2 (second and fourth row) and the bottom row of Fig. 3, constructed as described in Sec. II. This primitive model should approximate the polarization of the C–X  $\sigma$ -bond as well as the direct through-space effects of the substituents in the substituted benzene. More importantly, these additive ESPs reflect substituent effects on the ESP *not* due to changes in the aryl  $\pi$ -system, since the  $\pi$ -electron-density is that of unsubstituted benzene.

The similarities of the additive ESPs to the true ESPs in Fig. 2 are striking. Computed Hodgkin indices<sup>38</sup> further underscore the similarity of the additive and true ESPs, with most values of

**H** exceeding 0.95. For all substituents, the plots of the intact substituted benzenes are qualitatively similar to those derived from this simple additive model. Indeed, for several substituents the plots are indistinguishable (see, for example, phenylmethanol, thioanisole, benzenethiol, ethynylbenzene, and phenylsilane). For these systems in particular, changes in the ESP relative to that of benzene arise entirely from through-space effects.  $\pi$ -resonance cannot possibly play an appreciable role, since in the additive ESPs the aryl  $\pi$ -system is identical to that of unsubstituted benzene by construction.

There is some deviation between the additive ESPs and the true ESPs for several of the systems in Fig. 2. These deviations occur primarily for strong electron-donating or accepting substituents (OCH<sub>3</sub>, BF<sub>2</sub>, SiF<sub>3</sub>, NO, and NO<sub>2</sub>), suggesting that changes in the aryl  $\pi$ -system influence the molecular ESPs of these substituted systems. Similar behavior was observed previously<sup>31</sup> for the ESPs at a single point above the center of substituted benzenes. The observed deviations are in accord with standard resonance parameters for these substituents: for example, OH is a strong  $\pi$ -electron donor ( $R = -0.64$ ), and consequently the additive ESPs is more positive above the ring than for the true ESP. Conversely, NO is a strong  $\pi$ -electron-withdrawing group ( $R = 0.42$ ) and the additive ESP is more negative than the ESP for C<sub>6</sub>H<sub>5</sub>NO. The agreement between the additive ESPs and true ESPs for the aniline derivatives (Fig. 3) is generally slightly poorer (**H** = 0.78 to 0.95) than that observed for the substituents depicted in Fig. 2, in accord with the very strong  $\pi$ -donating character of substituted amines.

Contour plots of the ESP in a plane perpendicular to the aryl ring and passing through the *ipso* and *para* carbons are shown in Fig. 4 for benzene and five substituted benzenes (NH<sub>2</sub>, OH, CH<sub>3</sub>, F, and NO<sub>2</sub>). These plots, employing the same color-scheme as the surface maps shown in Fig. 2 and Fig. 3, offer an alternative, complementary view and enable a more complete comparison of the true ESPs with the additive ESPs. To clarify the connection between these contour plots and the ESP maps in Fig. 2 and Fig. 3, the electron density contour value used to construct the isodensity surfaces is superimposed on the ESP contour plots. Also shown in Fig. 4 are contour plots of the additive ESPs for these selected systems. There are small differences between the additive ESPs and the true ESPs. However, the values of the ESP in this plane are mimicked by the additive model and no changes in the  $\pi$ -electron-density are necessary to recover much of the substituent effect on the ESP. Specifically, for fluorobenzene, the regions of positive and negative ESP are roughly the same between the additive and true ESP plots. The primary difference is the very small region above the center of the ring where the ESP dips below  $-11.25$  kcal mol<sup>-1</sup> (red) visible in the true ESP but missing in the additive ESP (the additive ESP is  $-8.9$  kcal mol<sup>-1</sup> in this region). Similarly, for aniline the additive ESP overestimates the ESP above the ring, as was apparent in Fig. 3.

Electron density contour plots for these systems are also shown in Fig. 4. The electron densities are similar, as expected, apart from the area immediately surrounding the substituent. However,  $\pi$ -electron densities of aryl rings do change in response to introduced substituents. This can be most readily seen in contour plots of the difference in electron density between the substituted benzenes and benzene [*i.e.*:  $\Delta\rho = \rho(\text{C}_6\text{C}_5\text{X}) - \rho(\text{C}_6\text{H}_6)$ ]. Because the scale is chosen to showcase the densities differences around the *para* carbon, the  $\Delta\rho$  values immediately surrounding the substituent are far off the scale.

The changes in the electron density surrounding C<sub>para</sub> exhibit expected trends:  $\pi$ -donating substituents (NH<sub>2</sub>, OH, CH<sub>3</sub>, and F) show a net gain in density above and below the *para* carbon while  $\pi$ -accepting NO<sub>2</sub> reduces the electron density in this region. Despite these changes in the electron density surrounding the *para* carbon, the density above and below the *center* of the ring, is essentially unchanged in each of these systems. These density difference plots can be used to rationalize the differences between the additive ESP and true ESP contour plots. In the additive model, there is no change in the aryl  $\pi$ -system, so the effects of the density

differences above and below  $C_{para}$  will be neglected. For aniline, the overestimation of the ESP above  $C_{para}$  in the additive ESP is due to the neglect of the increase in  $\pi$ -electron density at the *para* carbon in the additive model. Similarly, the additive ESP of nitrobenzene slightly underestimates the ESP above the *para* carbon, consistent with the decrease in density in that region in the intact system that is not present in the additive model.

Since the additive ESPs are similar to the true ESP in each of these cases, it is clear that the effects of these  $\pi$ -electron density changes on the ESP are relatively minor. This is unsurprising, since these density changes are modest compared to the changes in the electron density surrounding the substituent. The through-space electrostatic effects of the substituents swamp the effect of  $\pi$ -donation and withdrawal, which in most cases shows up as a small perturbation of the ESP changes arising from non-resonance effects.

## B. Polysubstituted Benzenes

ESPs for three polysubstituted benzenes are presented in Fig. 5, along with additive ESPs. Computed Hodgkin indices again indicate a strong similarity between the true ESPs and the additive ESPs. These polysubstituted benzenes were recently studied by Ringer and Sherrill<sup>9</sup> in the context of the sandwich configuration of the benzene dimer. Ringer and Sherrill argued<sup>9</sup> that the ESP of the pictured rotamer of hexaaminobenzene “confirms an electron-rich  $\pi$  cloud” while  $C_6H_3(CN)_3$  and  $C_6F_6$  are similarly shown to have “noticeably depleted electron density in the center of the substituted rings.” The negative ESP above hexaaminobenzene and the positive ESP above tricyanobenzene and hexafluorobenzene do not necessarily arise from any change in the  $\pi$ -electron-density, since in the additive ESPs the aryl  $\pi$ -system is identical in each case. Labeling substituted aryl rings “ $\pi$ -electron-rich” or “ $\pi$ -electron-poor” based solely on computed ESP plots is clearly unfounded.

Hexafluorobenzene is of particular importance, since the reversed quadrupole moment of  $C_6F_6$ , compared to  $C_6H_6$ , is invoked to explain the strong face-to-face interaction of benzene and perfluorobenzene.<sup>4,39–43</sup> Perfluorobenzene also features in discussions of anion/ $\pi$  interactions<sup>44</sup> and in related complexes in which the  $\pi$ -cloud of  $C_6F_6$  purportedly serve as an electron acceptor.<sup>45</sup> The reversal in electrostatics of perfluorobenzene is sometimes attributed to the withdrawal of electron density from the center of the ring by the fluorines. However, Laidig<sup>46</sup> showed in 1991 that the quadrupole moment of  $C_6F_6$  arises primarily from the build-up of electron density along the periphery of the ring (*i.e.*: on the fluorines) rather than drastic changes of the electron density along the  $C_6$  symmetry axis.

Contour plots of the electron density and density difference versus benzene for  $C_6F_6$  are shown in Fig. 4, along with contour plots of the ESP and additive ESP. There is clearly a depletion of electron density above and below the plane of the benzene due to the six fluorines. However, the introduction of a large amount of density associated with the fluorines easily swamps the changes above and below the benzene plane. As seen in Fig. 4, the additive ESP of perfluorobenzene closely resembles the true ESP, demonstrating that the highly positive ESP above the center of the ring arises primarily from through-space effects of the fluorines, not any effect on the aryl  $\pi$ -system. Thus, while the  $\pi$ -electron-density of  $C_6F_6$  is depleted compared to benzene (See Fig. 4), the positive ESP above the ring is not evidence of this, but merely of the through-space electrostatic effects of the F substituents.

## C. Substituted Cryptolepines

Cryptolepine, an alkaloid from the West African shrub *Cryptolepis sanguinolenta*, is of interest as a lead for the development of both antimalarial and antitumor drugs.<sup>47–49</sup> Cytotoxicity of cryptolepine arises from its intercalation into DNA at non-alternating G-C sequences and inhibition of topoisomerase II.<sup>49,50</sup> The origin of the antimalarial activity is less well

understood, though it is thought to involve the inhibition of hemazoin formation, similar to chloroquine.<sup>47</sup> There are significant efforts to develop cryptolepine derivatives that offer comparable or exceptional antimalarial activity without the associated cytotoxicity. 7,9-dinitrocryptolepine has been shown to exhibit antimalarial activity in the absence of DNA-intercalation and toxicity, though the mode of antimalarial activity might differ from that of the parent compound.<sup>47,51</sup> Electrostatic interactions are expected to be important in both the DNA-intercalation and in the inhibition of hemazoin formation for substituted cryptolepines.<sup>52</sup> ESP plots of cryptolepine and dinitrocryptolepine are shown in Fig. 6. The two nitro groups have a profound effect on the ESP, with the most pronounced changes localized on the substituted ring. An additive ESP for 7,9-dinitrocryptolepine is included in Fig. 6(b), constructed by adding the ESP of cryptolepine with the ESP of two appropriately placed HNO<sub>2</sub> moieties. Because there are only very minor differences between the true ESP and the additive model ( $H = 1.00$ ), it is clear that the majority of the substituent effect arises from through-space effects. The  $\pi$ -system of cryptolepine plays a very minor role. In general, when considering ESPs of substituted analogs of candidate drugs built on aryl frameworks, the role of direct through-space effects of substituents is potentially significant and must be considered.

#### D. ESPs in Crystal Engineering and Host-Guest Chemistry

The field of supramolecular chemistry has blossomed in recent years, enabling the construction of complex molecular systems, molecular machines, and materials with novel properties through subtle control over intermolecular interactions.<sup>4,53</sup> Often this control arises from substituent effects on non-covalent interactions. In this regard plots of molecular electrostatic potentials are valuable tools. One example of host-guest systems for which ESP maps have been employed are the molecular tweezers of Klärner and co-workers.<sup>54–56</sup> Klärner *et al.* synthesized and characterized a series of molecular tweezers based on bimethylene “hinges” separated by a benzene bridge with polycyclic aromatic “arms”.<sup>54</sup> These receptors are powerful binders of what were described as “electron deficient” aryl systems.<sup>56</sup> The preferential binding was rationalized based on computed ESPs of the clips and the guest molecules (see Fig. 7a–b). It was noted that substituted aryl systems with more positive ESPs (*e.g.*: 1,8-DNAQ, 1,5-DNAQ, and TNF) are bound much more strongly than analogous systems with more negative ESPs (*e.g.*: AQ), due to the favorable electrostatic interactions with the predominantly negative ESPs of the inner walls of the tweezers in the former case. Additive ESP plots of 1,8-DNAQ, 1,5-DNAQ, and TNF are provided in Fig. 7c. In each case, the additive ESP is essentially indistinguishable from the true ESPs ( $H = 0.96 - 0.98$ ). These significant changes in the ESP arise almost entirely from through-space effects;  $\pi$ -resonance plays no discernable role.

Another example gleaned from the field of supramolecular chemistry exploits the avidity of arenes for perfluorinated arenes,<sup>4,39–43</sup> originally observed by Patrick and Prosser.<sup>40</sup> As mentioned in Sec. III.B, this favorable interaction results from the opposite sign but comparable magnitude of the quadrupole moments of benzene and hexafluorobenzene.<sup>39,57</sup> This strong attractive stacking interaction has led to the use of the C<sub>6</sub>H<sub>6</sub>  $\cdots$  C<sub>6</sub>F<sub>6</sub> interaction as a supramolecular synthon,<sup>58</sup> and this interaction has been exploited in countless systems. For example, Grubbs and co-workers<sup>43</sup> utilized perfluoroarene-arene interactions to achieve topological and stereochemical control over the photochemically driven reaction of 1,3-diynes in the condensed phase. Ponzini, Zaghera, Hardcastle, and Siegel<sup>59</sup> later demonstrated the utility of such interactions in the generation of highly ordered crystals of 1,3,5-trisphenethynylbenzene and 1,3,5-tris(perfluorophenethynyl)benzene (Scheme 3). In both of this system<sup>59</sup> and that studied by Grubbs and co-workers,<sup>43</sup> the electrostatic complementarity of the phenyl and perfluorophenyl moieties lead to highly-ordered alternating face-to-face stacks in mixed crystals, while the two components on their own form slipped-stacked arrangements.

ESPs of trisphenethynylbenzene and the fluorinated analog are shown in Fig. 8. The complementary nature of the ESP of the aryl and perfluoroaryl functionalities is immediately apparent. However, the additive ESP of the perfluorinated system (Fig. 8, far right) once again shows that the highly positive ESP above the center of perfluorinated aryl rings is reproduced without any changes in the aryl  $\pi$ -system ( $H = 0.78$ ).

#### IV. Implications for Non-Covalent Interactions with Aromatic Systems

Many qualitative models of substituent effects in non-covalent interactions with aromatic rings rest on the assumption that the dominant electrostatic effect arises from the polarization of the aryl  $\pi$ -system. This is most prominent in models of the benzene dimer advocated by Cozzi and Siegel<sup>60</sup> (the polar/ $\pi$  model) and Hunter and co-workers.<sup>7,42,61</sup> The crux of these primarily electrostatic models is that electron donors increase the aryl  $\pi$ -electron-density, increasing the electrostatic repulsion with the  $\pi$ -system of the non-substituted ring while electron acceptors enhance the benzene-benzene interaction through the opposite mechanism. While there have been numerous publications criticizing these models,<sup>9,27,28,62</sup> the underlying assumption that substituents modulate the electrostatic properties above the plane of benzene via polarization of the aryl  $\pi$ -system has previously remained largely unaddressed.

We have recently analyzed prototypical non-covalent interactions with substituted benzenes, including the sandwich and edge-to-face configurations of the benzene dimer<sup>63</sup> and the cation/ $\pi$  interaction of  $\text{Na}^+$  with  $\text{C}_6\text{H}_5\text{X}$ .<sup>31</sup> The primary conclusions were that direct through-space interactions of the substituents were the dominant cause of substituent effects.<sup>31,63</sup> The electrostatic component of these direct interactions is reflected in the current finding that variation in ESPs maps of substituted benzenes are due in large part to through-space effects of the substituents. Thus, all models of substituent effects in intermolecular arene interactions based on ESPs should similarly reflect the role of through-space effects. Given the prevalence of electrostatic models, there is a potential for a broad revision of our understanding of the effect of substituents in myriad systems. For example, in the perfluoroarene-arene interactions utilized in crystal engineering, the present results suggest that this strong interaction arises primarily from the direct interaction of the fluorines with the non-fluorinated ring, not  $\pi$ -polarization. Similarly, in the prototypical anion/ $\pi$  interaction between halide anions and  $\text{C}_6\text{F}_6$ ,<sup>44</sup> the favorable interaction is potentially due largely to direct through-space interactions, not a depleted  $\pi$ -system as generally assumed.<sup>44</sup> Indeed, Clements and Lewis<sup>64</sup> showed that the attractive interaction between halogenated benzenes and  $\text{F}^-$  is due to direct interactions with the substituents.

The present work is a clarion call for the reevaluation of models of substituent effects in non-covalent interactions in which ESP arguments are central, since often it was assumed that changes in arene ESPs reflect changes in the aryl  $\pi$ -system. Specifically, the previously underappreciated role of direct through-space interactions of substituents must be reconsidered.

#### V. Summary and Conclusions

Molecular electrostatic potentials are powerful tools for the interpretation and prediction of chemical phenomena and non-covalent interactions. However, deep-rooted misconceptions regarding the effect of substituents on the ESPs of substituted aromatic systems pervade the literature. Equating changes in ESPs with changes in the local electron density is prevalent, as exemplified by the “ $\pi$ -electron-rich” and “ $\pi$ -electron-poor” monikers assigned to aromatic systems often based solely on ESP plots. While substituents do perturb the aryl  $\pi$ -system, the effects of these changes on the electrostatic potential surrounding aromatic systems are often swamped by the significant changes in the electron densities associated with the substituents. Numerous publications<sup>65</sup> have demonstrated that most substituents have no significant effect



on the aromaticity of benzene. This resiliency of the benzene  $\pi$ -system shows up again in arene ESPs; for most substituents the polarization of the aryl  $\pi$ -cloud is modest, and does not significantly alter the ESP above the aromatic ring.

The role of through-space effects on ESPs was demonstrated here for a series of substituted benzenes and for more complex substituted arenes taken from disparate areas of research. Specifically, the change in the ESP of cryptolepine, a potent antimalarial and cytotoxic agent, induced by nitro substituents was shown to be independent of the aryl  $\pi$ -system. Similarly, the highly positive ESP values above the face of perfluorinated arenes, which are ubiquitous in supramolecular chemistry, can be reproduced with no alteration of the aryl  $\pi$ -system. Implications for our understanding of non-covalent interactions with substituted aromatic rings are profound, since substituent effects on the electrostatic component of many of these interactions arise primarily from direct interactions with the substituents.

Based on traditional,  $\pi$ -resonance-based models of non-covalent interactions with arenes, one would expect classical molecular mechanics force-fields to perform poorly for supramolecular assembly phenomena. This is because MM force-fields typically do not explicitly account for the perturbation of aryl  $\pi$ -systems by substituents. However, the present finding that polarization of the aryl  $\pi$ -system has minor effects on arene ESPs explains the often excellent performance of MM force-fields for  $\pi$ - $\pi$  interactions.<sup>66</sup> The neglect of changes in aryl  $\pi$ -systems by substituents is therefore warranted. Treatment of only direct interactions with the substituents should suffice.

A hallmark of chemistry is the development and widespread employment of qualitative predictive models. Electrostatic potential plots constitute a powerful tool in this regard, demonstrating utility in many areas of chemistry and molecular biology. Without a sound understanding of substituent effects on ESPs, the utility of these tools is handicapped. A counterintuitive yet striking demonstration of the dominance of through-space effects on ESPs of substituted arenes has been provided, with far-reaching implications for the understanding of non-covalent interactions in the fields of host-guest chemistry, crystal engineering, and rational drug design, among others. Perhaps most importantly, we have clearly shown that changes in ESPs do not necessarily reflect changes in the local electron density.

## Supplementary Material

Refer to Web version on PubMed Central for supplementary material.

## Acknowledgments

This work was supported by NIH-1F32GM082114 (S.E.W.) and NIH-GM36700 (K.N.H.). S.E.W. would like to thank H. Lischka for helpful suggestions and H. M. Jaeger and F. A. Evangelista for stimulating discussions regarding this work, which is dedicated to K. M. Williams and N. L. Wheeler. Computer time was provided in part by the UCLA Institute for Digital Research and Education (IDRE).

## References

1. Politzer, P.; Truhlar, DG. *Chemical Applications of Atomic and Molecular Electrostatic Potentials*. New York: Plenum; 1981. Murray, JS.; Sen, K. *Molecular Electrostatic Potentials: Concepts and Applications*. Elsevier Science; 1996. Naráy-Szabó G, Ferenczy GG. *Chem. Rev* 1995;95:829–847.
2. Politzer, P.; Murray, JS. *Computational Medical Chemistry for Drug Discovery*. Bultinck, P.; De Winter, H.; Langenaeker, W.; Tollenaere, JP., editors. New York: Marcel Dekker Inc; 2004. p. 213-234.
3. Politzer, P.; Murray, JS. *Reviews in Computational Chemistry*. Lipkowitz, KB.; Boyd, DB., editors. Vol. Vol. 2. New York: VCH Publishers; 1991.

4. Meyer EA, Castellano RK, Diederich F. *Angew. Chem. Int. Ed* 2003;42:1210–1250.
5. Mecozzi S, West AP Jr, Dougherty DA. *Proc. Natl. Acad. USA* 1996;93:10566–10571.
6. Gung BW, Amicangelo JC. *J. Org. Chem* 2006;71:9261–9270. [PubMed: 17137351]
7. Cockroft SL, Perkins J, Zonta C, Adams H, Spey SE, Low CMR, Vinter JG, Lawson KR, Urch CJ, Hunter CA. *Org. Biomol. Chem* 2007;5:1062–1080. [PubMed: 17377660]
8. Hohenstein EG, Sherrill CD. *J. Phys. Chem. A* 2009;113:878–886. [PubMed: 19132847]
9. Ringer AL, Sherrill CD. *J. Am. Chem. Soc* 2009;131:4574–4575. [PubMed: 19278258]
10. Naráy-Szabó, G. *Molecular Electrostatic Potentials: Concepts and Applications*. Murray, JS.; Sen, K., editors. Berlin: Elsevier; 1996. p. 333–365. RP A, B L, SL P, JG V. *J. Comput. Aided Mol. Des* 1995;9:33–43. [PubMed: 7751868] Sheinerman FB, Honig B. *J. Mol. Biol* 2002;318:161–177. [PubMed: 12054776]
11. Zheng H, Comeforo K, Gao J. *J. Am. Chem. Soc* 2009;131:18–19. [PubMed: 19067509]
12. Galabov B, Ilieva S, Schaefer HF. *J. Org. Chem* 2006;71:6382–6387. [PubMed: 16901119] Suresh CH, Gadre SR. *J. Phys. Chem. A* 2007;111:710–714. [PubMed: 17249762] Gadre SR, Suresh CH. *J. Org. Chem* 1997;62:2625–2627. [PubMed: 11671606] Suresh CH, Gadre SR. *J. Am. Chem. Soc* 1998;120:7049–7055.
13. Politzer P, Murray JS. *J. Mol. Struct* 1996;376:419–424. Murray JS, Lane P, Politzer P, Bolduc PR. *Chem. Phys. Lett* 1990;168:135–139. Rice BM, Hare, J J. *J. Phys. Chem. A* 2002;106:1770–1783.
14. Chana A, Concejero MA, de Frutos M, González MJ, Herradó B. *Toxicology* 2002;15:1514–1526.
15. For recent examples, see Yearley EJ, Zhurova EA, Zhurov VV, Pinkerton AA. *J. Am. Chem. Soc* 2007;129:15013–15021. [PubMed: 17994745] and Zhurova EA, Matta CF, Wu N, Zhurov VV, Pinkerton AA. *J. Am. Chem. Soc* 2006;128:8849–8861. [PubMed: 16819879]
16. Scrocco, E.; Tomasi, J. *Topics in Current Chemistry*. Vol. 42. Berlin: Springer; 1973. p. 95–170. Scrocco E, Tomasi J. *Adv. Quant. Chem* 1978;11:115–193. Bonaccorsi R, Scrocco E, Tomasi J. *J. Chem. Phys* 1970;52:5270–5284. Bonaccorsi R, Scrocco E, Tomasi J. *Theor. Chim. Acta* 1971;21:17–27. Bonaccorsi R, Pullman A, Scrocco E, Tomasi J. *Chem. Phys. Lett* 1972;12:622–624. Bonaccorsi R, Pullman A, Scrocco E, Tomasi J. *Theor. Chim. Acta* 1972;24:51–60. Berthier G, Bonaccorsi R, Scrocco E, Tomasi J. *Theor. Chim. Acta* 1972;26:101–105. Tomasi, J.; Mennucci, B.; Cammi, R. *Molecular Electrostatic Potentials: Concepts and Applications*. Murray, JS.; Sen, K., editors. Berlin: Elsevier; 1996. p. 1–85.
17. Yook I, Benítez D, Miljanić OŠ, Zhao Y-L, Tkatchouk E, Goddard WA III, Stoddart JF. *Cryst. Growth Des* 2009;9:2300–2309.
18. For recent examples, see Zhang Y, Luo M, Schramm VL. *J. Am. Chem. Soc* 2009;131:4685–4694. [PubMed: 19292447] Laughrey ZR, Kiehna SE, Riemen AJ, Waters ML. *J. Am. Chem. Soc* 2008;130:14625–14633. [PubMed: 18844354] Wang Y, Stretton AD, McConnell MC, Wood PA, Parsons S, Henry JB, Mount AR, Galow TH. *J. Am. Chem. Soc* 2008;129:13193–13200. [PubMed: 17918939] Terraneo G, Potenza D, Canales A, Jiménez-Barbero J, Baldrige KK, Bernardi A. *J. Am. Chem. Soc* 2007;129:2890–2900. [PubMed: 17309255] and Gortea V, Bollot G, Mareda J, Perez-Velasco A, Matile S. *J. Am. Chem. Soc* 2006;128:14788–14789. [PubMed: 17105272]
19. Anslyn, EV.; Dougherty, DA. *Sausalito, California: University Science Books; 2006. p. 14–15.*
20. Shusterman GP, Shusterman AJ. *J. Chem. Ed* 1997;74:771–776.
21. Hammett LP. *Chem. Rev* 1935;17:125–136. Hammett, LP. *Physical Organic Chemistry*. New York: McGraw-Hill; 1940.
22. Charton M. *Prog. Phys. Org. Chem* 1981;13:120–251.
23. Hansch C, Leo A, Taft RW. *Chem. Rev* 1991;91:165–195.
24. Roberts JD, Moreland WT. *J. Am. Chem. Soc* 1953;75:2167–2173.
25. Taft RW. *J. Phys. Chem* 64:1805–1815. 64.
26. Swain CG, Lupton EC. *J. Am. Chem. Soc* 1968;90:4328–4337.
27. Sinnokrot MO, Sherrill CD. *J. Phys. Chem. A* 2003;107:8377–8379. Sinnokrot MO, Sherrill CD. *J. Phys. Chem. A* 2006;110:10656–10668. [PubMed: 16970354]
28. Ringer AL, Sinnokrot MO, Lively RP, Sherrill CD. *Chem. Eur. J* 2006;12:3821–3828.
29. Arnstein SA, Sherrill CD. *Phys. Chem. Chem. Phys* 2008;10:2646–2655. [PubMed: 18464979]

30. Ma JC, Dougherty DA. *Chem. Rev* 1997;97:1303–1324. [PubMed: 11851453] Mecozzi S, West AP Jr, Dougherty DA. *J. Am. Chem. Soc* 1996;118:2307–2308.
31. Wheeler SE, Houk KN. *J. Am. Chem. Soc* 2009;131:3126–3127. [PubMed: 19219986]
32. Klärner F-G, Polkowska J, Panitzky J, Seelbach UP, Burkert U, Kamieth M, Baumann M, Wigger AE, Boese R, Bläser D. *Eur. J. Org. Chem* 2004:1405–1423.
33. Politzer P, Lane P, Jayasuriya K, Domelsmith LN. *J. Am. Chem. Soc* 1987;109:1899–1901.
34. Becke AD. *J. Chem. Phys* 1993;98:5648–5652. Hehre WJ, Ditchfield R, Pople, A J. *J. Chem. Phys* 1972;56:2257–2261.
35. Frisch, MJ.; Trucks, GW.; Schlegel, HB.; Scuseria, GE.; Robb, MA.; Cheeseman, JR.; Montgomery, JA., Jr; Vreven, T.; Kudin, KN.; Burant, JC.; Millam, JM.; Iyengar, SS.; Tomasi, J.; Barone, V.; Mennucci, B.; Cossi, M.; Scalmani, G.; Rega, N.; Petersson, GA.; Nakatsuji, H.; Hada, M.; Ehara, M.; Toyota, K.; Fukuda, R.; Hasegawa, J.; Ishida, M.; Nakajima, T.; Honda, Y.; Kitao, O.; Nakai, H.; Klene, M.; Li, X.; Knox, JE.; Hratchian, HP.; Cross, JB.; Bakken, V.; Adamo, C.; Jaramillo, J.; Gomperts, R.; Stratmann, RE.; Yazyev, O.; Austin, AJ.; Cammi, R.; Pomelli, C.; Ochterski, JW.; Ayala, PY.; Morokuma, K.; Voth, GA.; Salvador, P.; Dannenberg, JJ.; Zakrzewski, VG.; Dapprich, S.; Daniels, AD.; Strain, MC.; Farkas, O.; Malick, DK.; Rabuck, AD.; Raghavachari, K.; Foresman, JB.; Ortiz, JV.; Cui, Q.; Baboul, AG.; Clifford, S.; Cioslowski, J.; Stefanov, BB.; Liu, G.; Liashenko, A.; Piskorz, P.; Komaromi, I.; Martin, RL.; Fox, DJ.; Keith, T.; Al-Laham, MA.; Peng, CY.; Nanayakkara, A.; Challacombe, M.; Gill, PMW.; Johnson, B.; Chen, W.; Wong, MW.; Gonzalez, C.; Pople, JA. Wallingford CT: Gaussian, Inc; 2004. Gaussian 03, Revision C.02
36. Pettersen EF, Goddard TD, Huang CC, Couch GS, Greenblatt DM, Meng EC, Ferrin TE. *J. Comput. Chem* 2004;25:1605–1612. [PubMed: 15264254]
37. If these additive ESPs are instead mapped onto an analogously derived additive electron density isosurface the results are indistinguishable from the present results
38. Hodgkin EE, Richards WG. *Int. J. Quant. Chem* 1987;32:105–110.
39. Battaglia MR, Buckingham AD, Williams JH. *Chem. Phys. Lett* 1981;78:421–423. Vrbancich J, Ritchie GLD. *Chem. Phys. Lett* 1983;94:63–68.
40. Patrick CR, Prosser GS. *Nature* 1960;187:1021–1021.
41. Dahl T. *Acta. Chem. Scand* 1988;42:1–7. West AP Jr, Mecozzi S, Dougherty DA. *J. Phys. Org. Chem* 1999;10:347–350.
42. Hunter CA, Lawson KR, Perkins J, Urch CJ. *J. Chem. Soc., Perkin Trans* 2001;2:651–669.
43. Coates GW, Dunn AE, Henling LM, Dougherty DA, Grubbs RH. *Angew. Chem. Chem. Int. Ed. Engl* 1997;36:248–251. Coates GW, Dunn AE, Henling LM, Ziller JW, Lobkovsky EB, Grubbs RH. *J. Am. Chem. Soc* 1998;120:3641–3649.
44. Ballester P. *Struct. Bond* 2008;129:127–174. Mascal M, Armstrong A, Bartberger DM. *J. Am. Chem. Soc* 2002;124:6274–6276. [PubMed: 12033854] Alkorta I, Rozas I, Elguero J. *J. Am. Chem. Soc* 2002;124:8593–8598. [PubMed: 12121100] Quiñero D, Garau C, Rotger C, Frontera A, Ballester P, Costa A, Deyà PM. *Angew. Chem. Chem. Int. Ed* 2002;41:3389–3392. Berryman OB, Bryantsev VS, Stay DP, Johnson DW, Hay BP. *J. Am. Chem. Soc* 2007;129:48–58. [PubMed: 17199282]
45. Gallivan JP, Dougherty DA. *Org. Lett* 1999;1:103–105. [PubMed: 10822544] Alkorta I, Rozas I, Elguero J. *J. Org. Chem* 1997;62:4687–4691. Danten Y, Tassaing T, Besnard M. *J. Phys. Chem. A* 1999;103:3530–3534.
46. Laidig K. *Chem. Phys. Lett* 1991;185:483–489.
47. Wright CW, Addae-Kyereme J, Breen AG, Brown JE, Cox MF, Croft SL, Gokcek Y, Kendrick H, Phillips RM, Pollet P. *J. Med. Chem* 2001;44:3187–3194. [PubMed: 11543688]
48. Wright C. *J. Pharm. Pharmacol* 2007;59:899–904. [PubMed: 17637183]
49. Bonjean K, De Pauw-Gillet MC, Defresne MP, Colson P, Houssier C, Dassonneville L, Bailly C, Greimers R, Wright C, Quetin-Leclercq J, Tits M, Angenot L. *Biochem* 1998;37:5136–5146. [PubMed: 9548744]
50. Lisgarten JN, Coll M, Portugal J, Wright CW, Aymami J. *Nat. Struct. Biol* 2002;9:57–60. [PubMed: 11731803]
51. Lisgarten JN, Potter BS, Palmer RA, Pitts JE, Wright CW. *J. Chem. Crystallogr* 2008;38:815–819.

52. Bhattacharya AK, Karle JM. *J. Med. Chem* 1966;39:4622–4629. Bhattacharya AK. *J. Mol. Struct. THEOCHEM* 2000;529:193–201. Medhi C, Mitchell JBO, Price SL, Tabor AB. *Biopolymers* 2000;52:84–93. [PubMed: 10898854]
53. Lehn JM. *Science* 1993;260:1762–1763. [PubMed: 8511582]
54. Klärner F-G, Kahlert B. *Acc. Chem. Res* 2003;36:919–932. [PubMed: 14674783]
55. Kamieth M, Klärner F-G, Diederich F. *Angew. Chem. Chem. Int. Ed* 1998;37:3303–3306. Klärner F-G, Panitzky J, Preda D, Scott LT. *J. Mol. Model* 2000;6:318–327.
56. Branchi B, Balzani V, Ceroni P, Campañá Kuchenbrandt M, Klärner F-G, Bläser D, Boese R. *J. Org. Chem* 2008;73:5839–5851. [PubMed: 18611052]
57. Williams J. *Acc. Chem. Res* 1993;26:593–598.
58. Thalladi VR, Goud S, Hoy VJ, Allen FH, Howard JAK, Desiraju GR. *Chem. Comm* 1996:401–402.
59. Ponzini F, Zagha R, Hardcastle K, Siegel JS. *Angew. Chem. Chem. Int. Ed* 2000;39:2323–2325.
60. Cozzi F, Annunziata R, Benaglia M, Baldrige KK, Aguirre G, Estrada J, Sritana-Anant Y, Siegel JS. *Phys. Chem. Chem. Phys* 2008;10:2686–2694. [PubMed: 18464983] Cozzi F, Cinquini M, Annunziata R, Dwyer T, Siegel JS. *J. Am. Chem. Soc* 1992;114:5729–5733.
61. Hunter CA, Sanders JKM. *J. Am. Chem. Soc* 1990;112:5525–5534.
62. Müller-Dethlefs K, Hobza P. *Chem. Rev* 2000;100:143–168. [PubMed: 11749236] Sinnokrot MO, Sherrill CD. *J. Am. Chem. Soc* 2004;126:7690–7697. [PubMed: 15198617] Lee EC, Kim D, Jurečka P, Tarakeshwar P, Hobza P, Kim KS. *J. Phys. Chem. A* 2007;111:3446–3457. [PubMed: 17429954] Grimme S. *Angew. Chem. Chem. Int. Ed* 2008;47:3430–3434.
63. Wheeler SE, Houk KN. *J. Am. Chem. Soc* 2008;130:10854–10855. [PubMed: 18652453] Wheeler SE, Houk KN. *Mol. Phys* 2009;107:749–760. [PubMed: 20046948]
64. Clements A, Lewis MJ. *J. Phys. Chem. A* 2006;110:12705–12710. [PubMed: 17107123]
65. Campanelli AR, Domenicano A, Ramonda F. *J. Phys. Chem. A* 2003;107:6429–6440. Krygowski TM, Ejsmont K, Stepień BT, Cyrański MK, Poater J, Solà M. *J. Org. Chem* 2004;69:6634–6640. [PubMed: 15387585] Krygowski TM, Stepień BT. *Chem. Rev* 2005;105:3482–3512. [PubMed: 16218559] Krygowski TM, Szatyłowicz H. *Trends Org. Chem* 2006;11:37–53. Wu JI, Pöhlhofer FG, Schleyer PvR, Puchta R, Kiran B, Mauksch M, Hommes NJRvE, Alkorta I, Elguero J. *J. Phys. Chem. A* 2009;113:6789–6794. [PubMed: 19472981]
66. Paton RS, Goodman JM. *J. Chem. Inf. Model* 2009;49:944–955. [PubMed: 19309094]

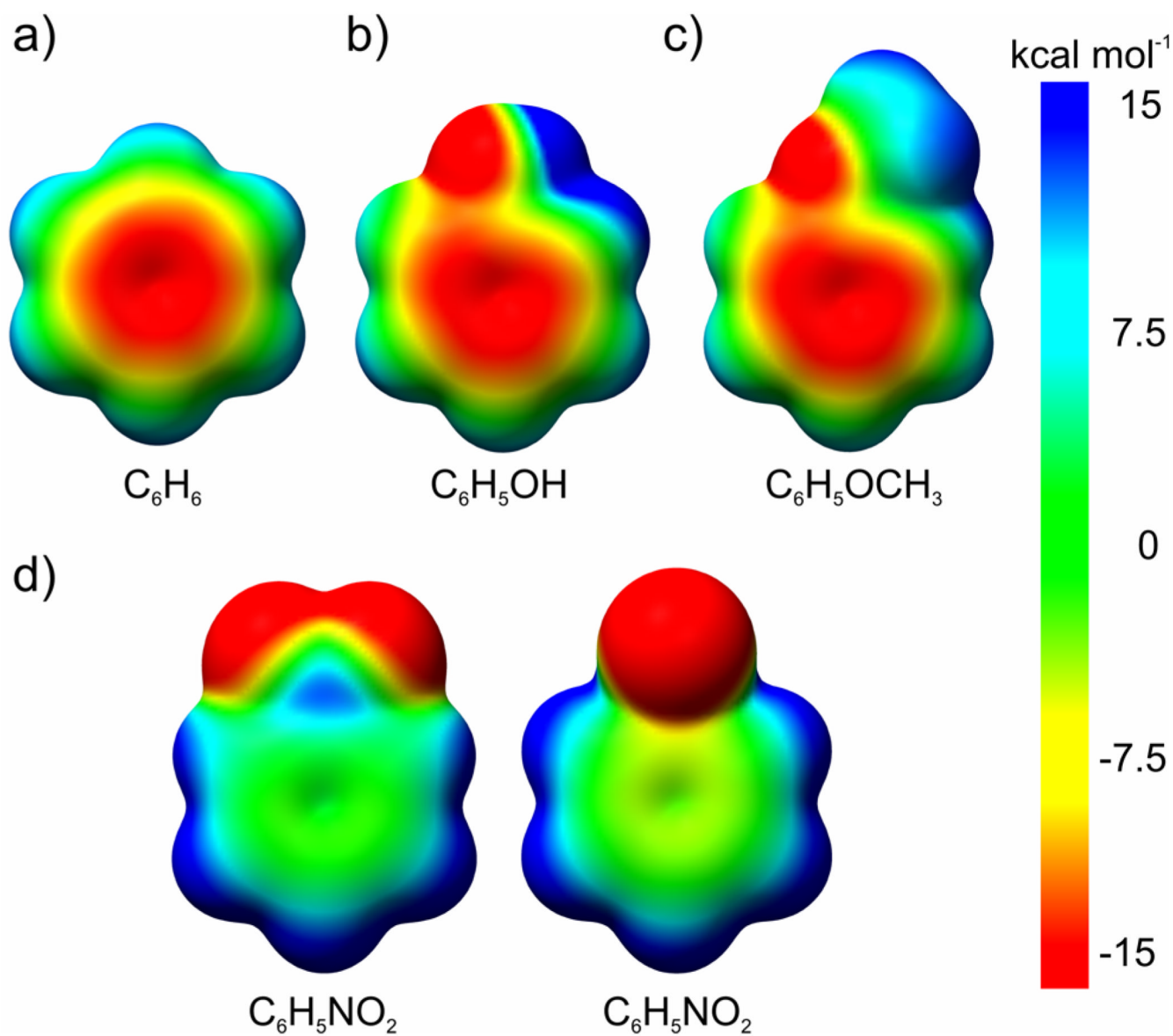


**Figure 1.** Plots of the electrostatic potential of (a) benzene, (b) phenol, (c) anisole, and (d) planar nitrobenzene (left) and perpendicular nitrobenzene (right), mapped onto electron density isosurfaces ( $0.001 \text{ e/au}^3$ )

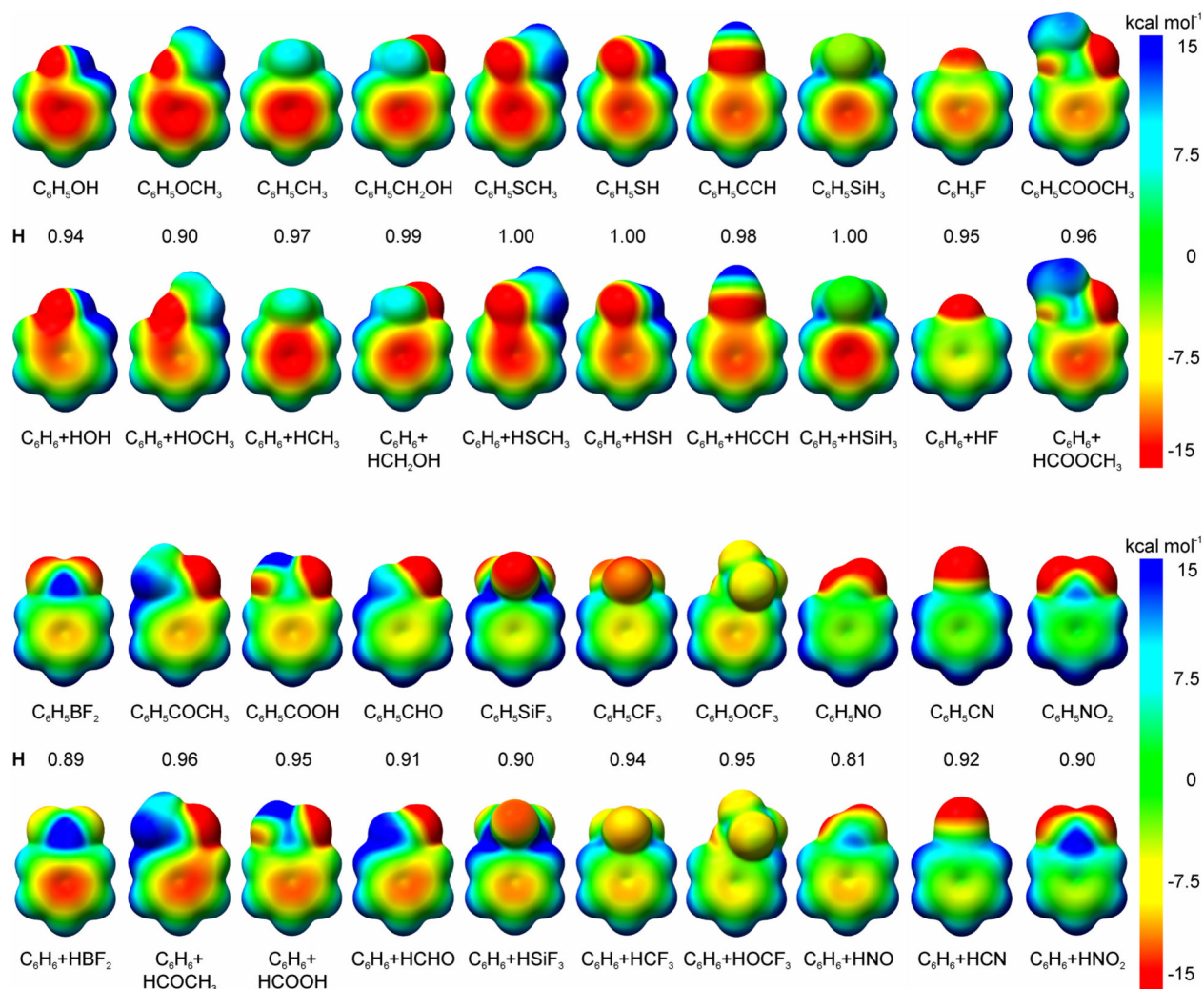


**Figure 2.** Plots of electrostatic potentials of monosubstituted benzenes (first and third row) and corresponding additive ESPs (second and fourth row). In each case, ESPs are mapped on electron density isosurfaces ( $0.001 \text{ e/au}^3$ ) for the substituted benzene. The Hodgkin similarity index (**H**) is computed for the ESP values on the isodensity surfaces for the true and additive ESPs.

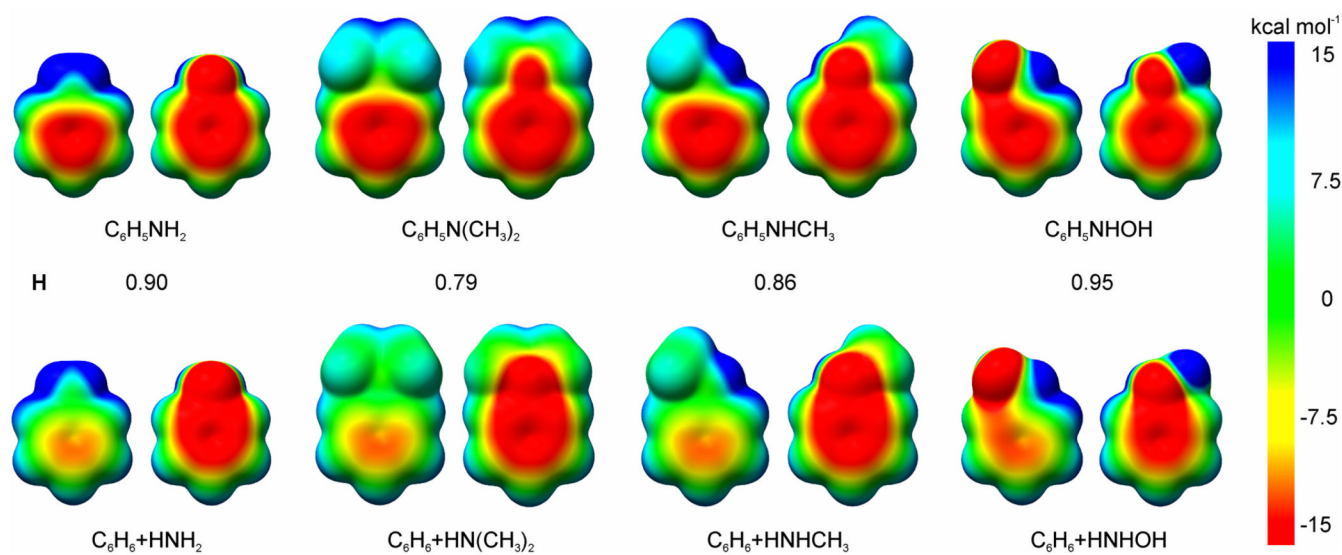


**Figure 3.** Front and back views of electrostatic potentials of aniline derivatives (top row) and corresponding additive ESPs (bottom row). ESPs are mapped on electron density isosurfaces ( $0.001 \text{ e/au}^3$ ) for the substituted benzene. The Hodgkin similarity index ( $H$ ) is computed for the ESP values on the isodensity surfaces for the true and additive ESPs.

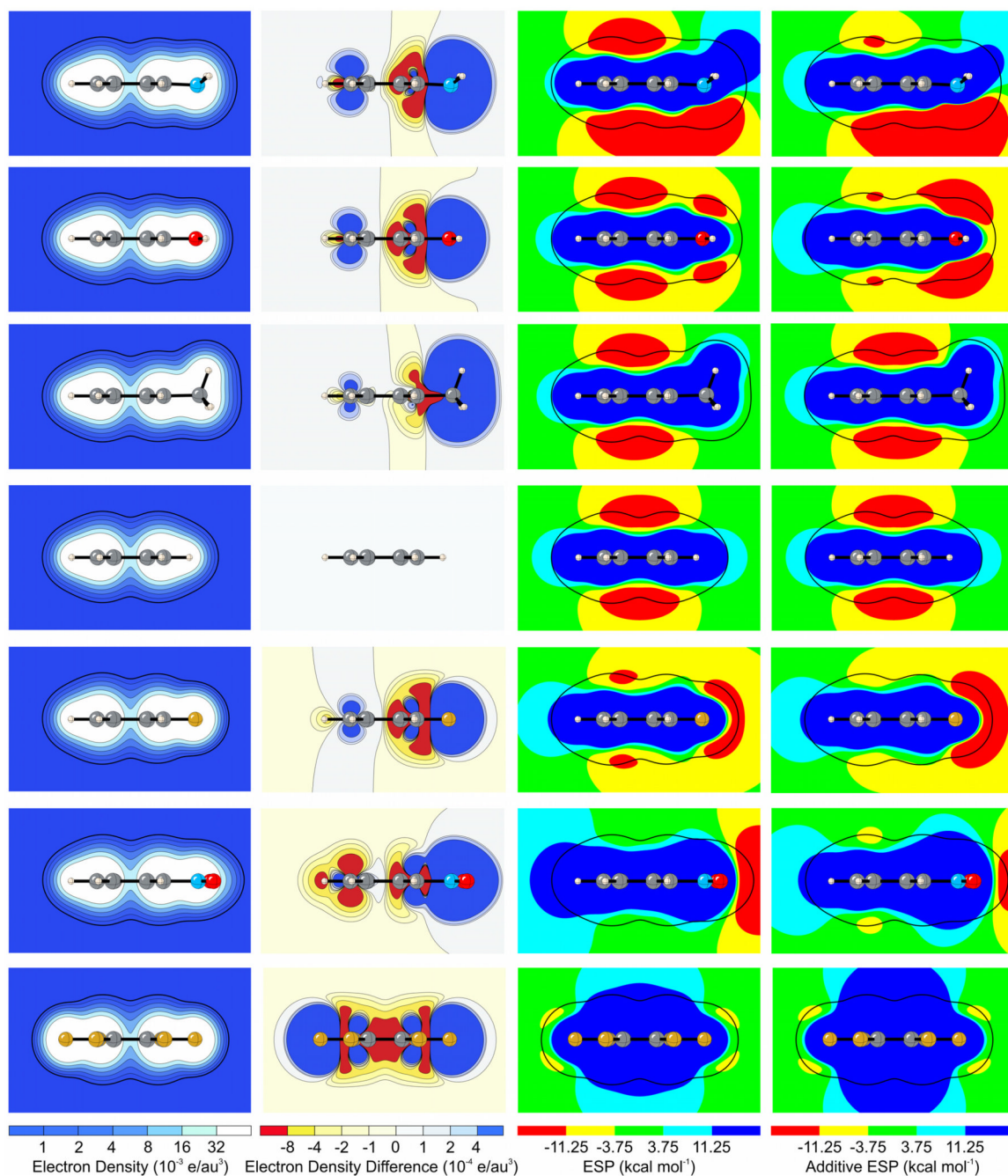


**Figure 4.**

Contour plots of the electron density, electron density difference versus benzene [ $\Delta\rho = \rho(\text{C}_6\text{H}_5\text{X}) - \rho(\text{C}_6\text{H}_6)$ ], electrostatic potential, and additive ESP for aniline, phenol, toluene, benzene, fluorobenzene, nitrobenzene, and hexafluorobenzene. The thick black line in the density and ESP plots denotes the electron density contour ( $0.001 \text{ e/au}^3$ ) used to construct the isodensity surfaces in Fig. 2 and Fig. 3.



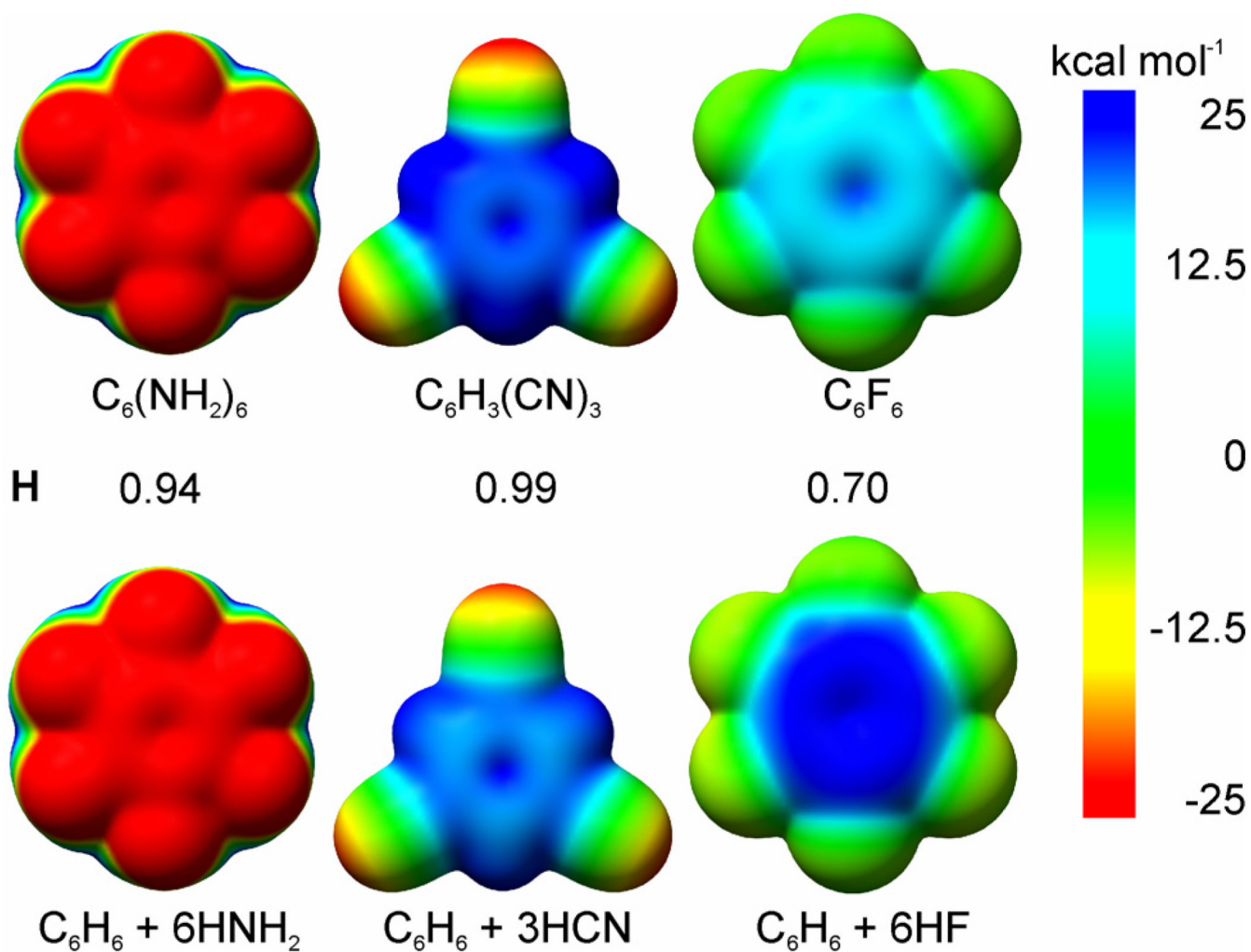


**Figure 5.** Plots of electrostatic potential of polysubstituted benzenes (top) and corresponding additive ESPs (bottom). In each case, ESPs are mapped onto electron density isosurfaces ( $0.001 \text{ e}/\text{au}^3$ ) for the substituted benzene. The Hodgkin similarity index (**H**) is computed for the ESP values on the isodensity surfaces for the true and additive ESPs.

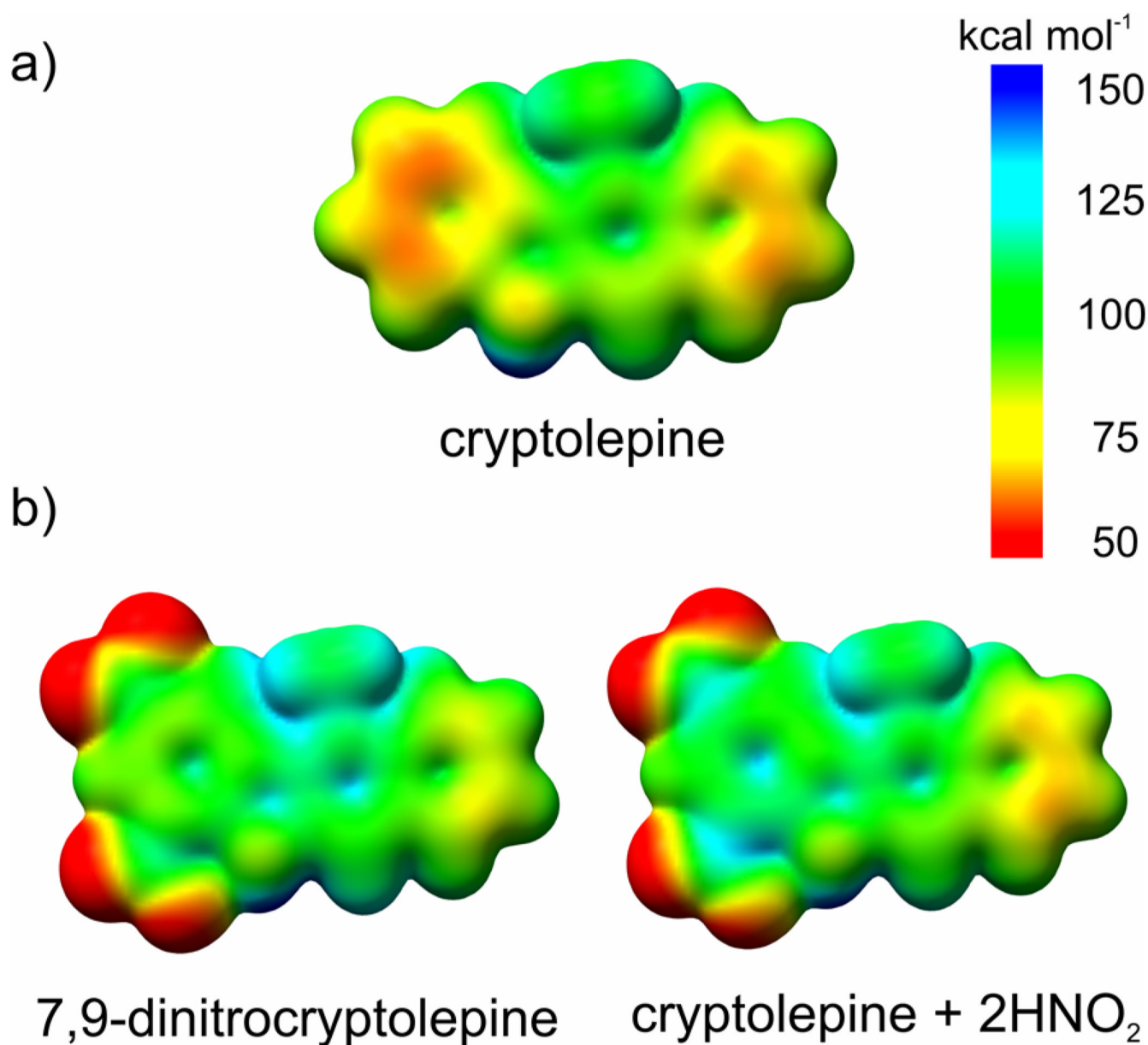


**Figure 6.**

(a) Electrostatic potential of cryptolepine; (b) ESP of 7,9-dinitrocryptolepine and additive ESP of 7,9-dinitrocryptolepine constructed by adding the ESP of cryptolepine with the ESP of two HNO<sub>2</sub> molecules and mapped onto the electron density isosurface of dinitrocryptolepine. Density isosurfaces correspond to  $\rho = 0.005 \text{ e/au}^3$ . The Hodgkin index for the true and additive ESP plots is 1.00.

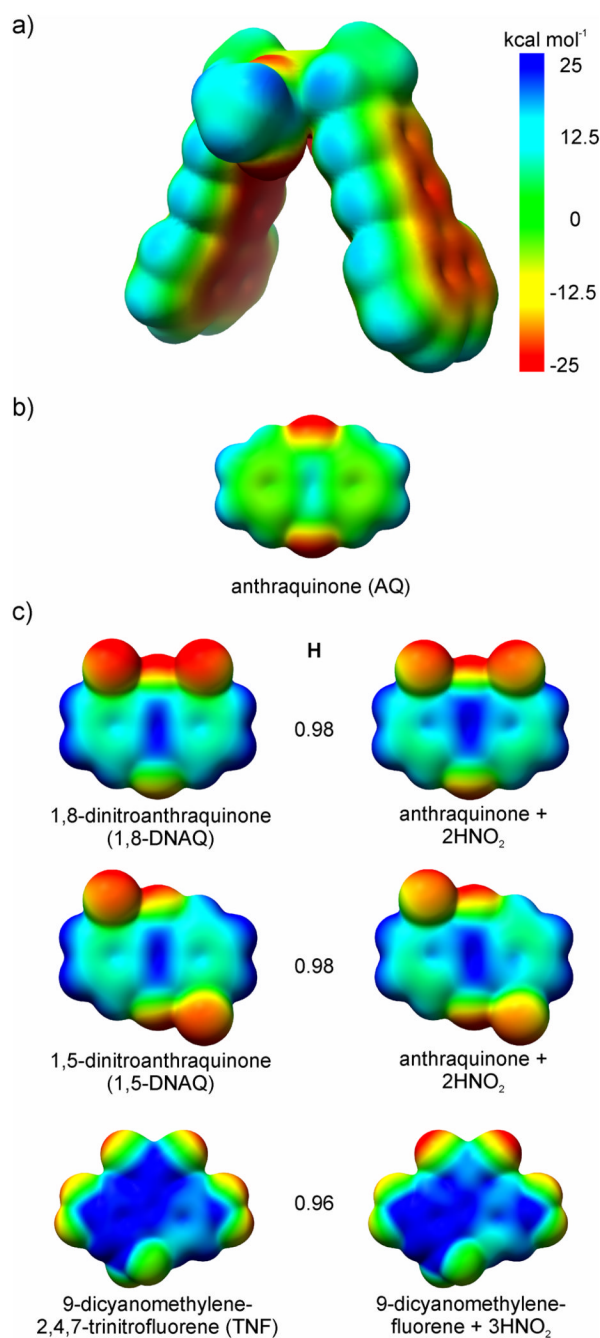


**Figure 7.** (a) ESP of molecular tweezers of Klärner and co-workers;<sup>54,56</sup> (b) ESP of anthraquinone; (c) ESPs (left) and additive ESPs (right) of two dinitroanthraquinones and 9-dicyanomethylene-2,4,5-trinitrofluorene. Density isosurfaces correspond to  $\rho = 0.001 \text{ e/au}^3$ . The Hodgkin similarity index (**H**) is computed for the ESP values on the isodensity surfaces for the true and additive ESPs.

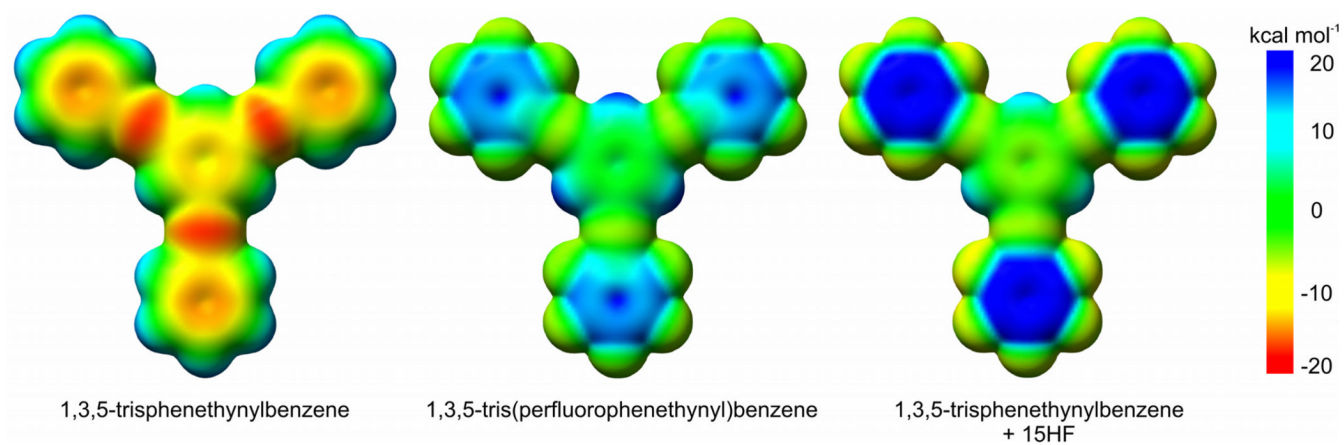
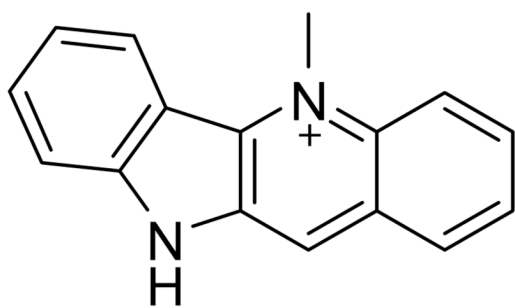
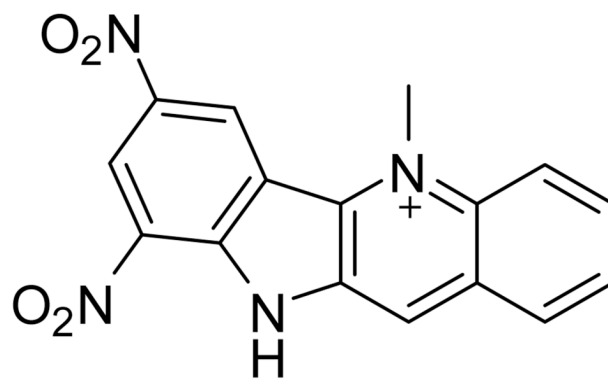


**Figure 8.** ESP plot of 1,3,5-trisphenethylbenzene (left) and plot of the true (middle) and additive (right) ESP of 1,3,5-tris(perfluorophenethyl)benzene, mapped onto electron density isosurfaces ( $0.001 \text{ e}/\text{au}^3$ ). The Hodgkins similarity index for the true and additive ESP plots is 0.78.

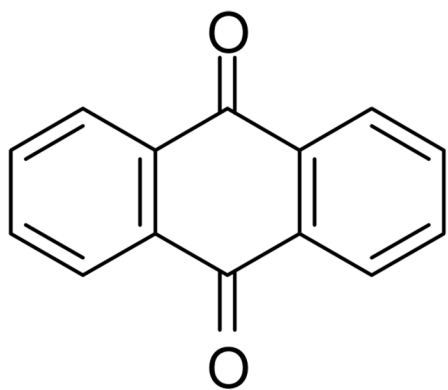


Cryptolepine

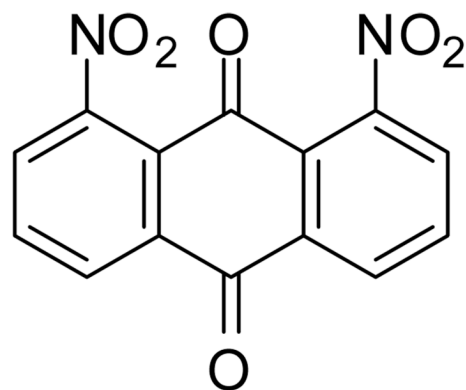


7,9-dinitrocryptolepine

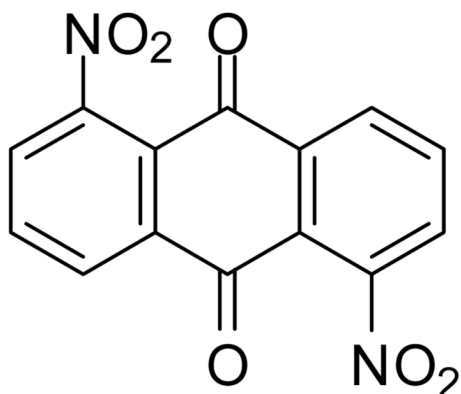
Scheme 1.



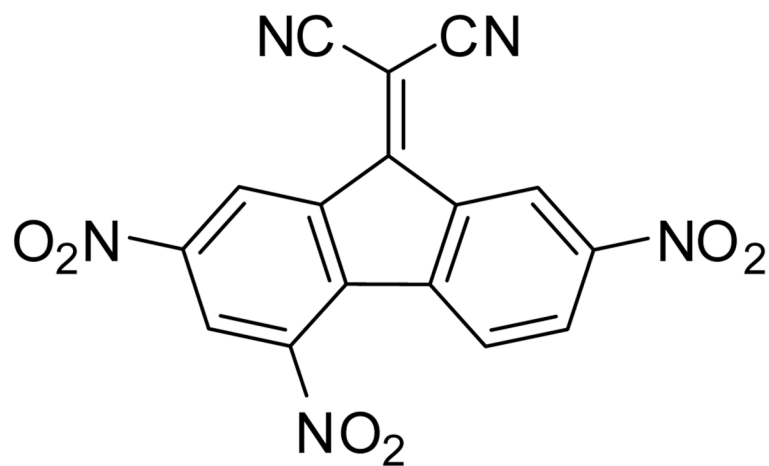
anthraquinone (AQ)



1,8-dinitroanthraquinone (1,8-DNAQ)

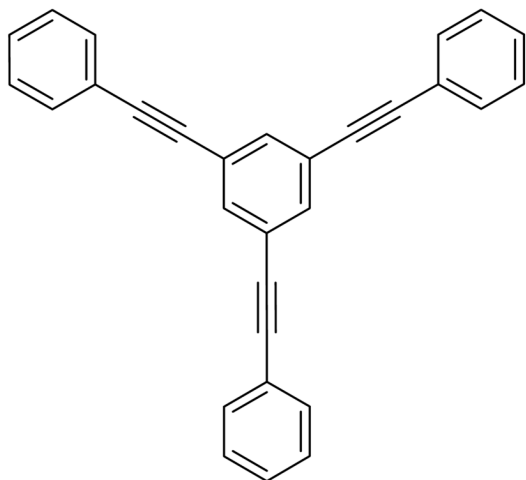


1,5-dinitroanthraquinone (1,5-DNAQ)



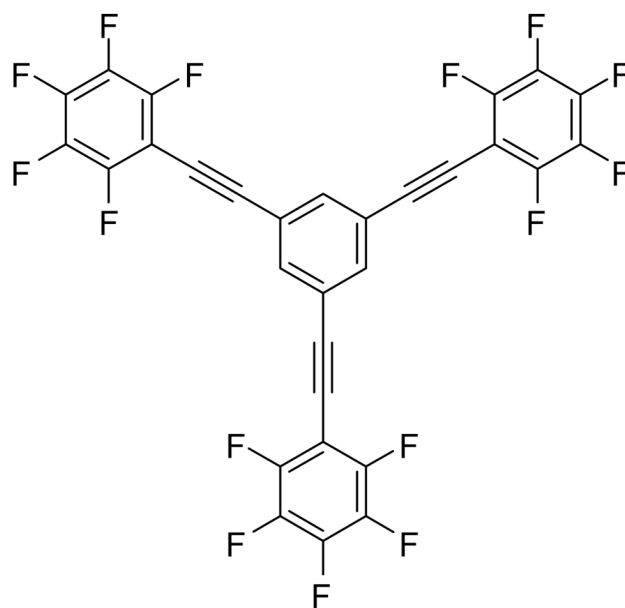
9-dicyanomethylene-2,4,7-trinitrofluorene (TNF)

Scheme 2.



1,3,5-trisphenylethynylbenzene

Scheme 3.



1,3,5-tris(perfluorophenylethynyl)benzene